Time-domain Analysis of Flutter in Long-span Cable-stayed Bridges

Yongyi Yang [1], Xiao Huang[2,*]

[1]XIHUA University, Chengdu, Sichuan 610031, China
[2]Yunnan Provincial Academy of Science and Technology (YAST), Kunming, Yunnan, 650106, China

* Corresponding author. yky2022488@163.com

Abstract. Bridge flutter is a forced vibration induced by the turbulent component in the natural atmosphere. It is a limit cycle oscillation that does not cause catastrophic structural failure. However, it occurs frequently, and prolonged vibrations can lead to fatigue damage in structural components. Excessive amplitude or acceleration may cause discomfort to pedestrians, jeopardize high-speed traffic safety, and even result in structural strength failure. In this chapter, flutter analysis is conducted for the Hanjiatuo Yangtze River Bridge on the Yuli Line. Based on the calculation of the structural natural frequencies, a comparison between frequency domain and time domain flutter analysis methods is performed to validate the reliability of the time domain analysis method for the wind-bridge system established in this study.

Keywords: able-stayed, Time-domain, Flutter, Stochastic wind field

1 Introduction

The phenomenon of flutter in long-span bridges, a type of forced vibration induced by natural atmospheric turbulence, is both common and significant. This kind of vibration is characterized by its limited amplitude and does not directly lead to catastrophic damage to the bridge structure. However, this does not imply that we can neglect its existence. Even with limited amplitude, frequent and persistent vibrations can cause fatigue in bridge components, such prolonged wear and tear may ultimately affect the bridge's lifespan and safety. Moreover, excessive flutter amplitudes or accelerations can also have adverse effects on bridge users. For pedestrians, it can cause physical discomfort, greatly reducing the user experience of the bridge. For vehicles traveling at high speed, the flutter phenomenon may pose a threat to driving safety. Especially under adverse weather conditions, this impact could be even more severe. Therefore, the issue of flutter response in long-span bridges is regarded as an important research topic in the current field of bridge wind engineering[1-5]. We need a profound understanding and in-depth study of it to find effective solutions to ensure the normal operation of the bridge and the safety of users. From design and construction to maintenance stages, we need to stay highly alert to the issue of flutter and adopt proactive measures to address it.

The aerodynamic admittance function, as the transfer function between pulsating flow and vibration force in terms of amplitude and phase, plays a pivotal role. It is the key parameter for accurately calculating the vibration time-domain load, a notion that has been supported and substantiated by numerous research findings [6-7]. In some specific scenarios, such as for streamlined sections, the aerodynamic admittance can be represented using the Sears function. This is because the airflow characteristics of streamlined sections are relatively regular and simple, without involving complex flow separation phenomena, hence the Sears function can provide a good description in these cases. However, when dealing with more complex situations, such as blunt sections, due to the complex flow separation phenomena involved, the simple Sears function can no longer meet the requirements. In such cases, we need to introduce a more accurate and comprehensive model to characterize the aerodynamic admittance, which necessitates considering the influence of the three-dimensional aerodynamic admittance function. The three-dimensional aerodynamic admittance function can more realistically reflect the behavior of the fluid in complex situations, providing us with a higher-level tool for understanding and mastering complex flow phenomena[8-9].

This paper, using the Hanjiatuo Yangtze River Bridge of the Chongqing-Lichuan Railway with a main span of 432m as the engineering background, has carried out numerical calculations on the flutter response of the Hanjiatuo Yangtze River Bridge using the time-domain method under the circumstances of considering the Sears function, considering the three-dimensional aerodynamic admittance function, and not considering the aerodynamic admittance. It analyses the impact of different functions on bridge flutter. By comparing with the frequency-domain analysis results, the correctness of the flutter time-domain analysis is validated.

2   Structural Dynamic Characteristics

According to the design information, a spatial finite element model was established for the analysis of the Hanjiatuo Yangtze River Bridge. In the finite element modeling, spatial beam elements were used for all components of the bridge towers. For the variable cross-section tower columns, the geometric properties of the central section of the element were used. The tower cables were made of C50 concrete, with an elastic modulus of 3.55×10^4 MPa, a Poisson's ratio of 0.2, and a material density of 2600 kg/m^3. The main beam truss members were modeled using spatial beam elements and made of steel. The elastic modulus was taken as 2.10×10^5 MPa, the Poisson's ratio was 0.3, and the material density was $7850 \times (1+25\%) = 9812.5$ kg/m^3. The material density of the bridge deck system and transverse beams was $7850 \times (1+8\%) = 8478$ kg/m^3. The inclined cables were simulated using bar elements, with an elastic modulus of 2.05×10^5 MPa, a Poisson's ratio of 0.3, a material density of 8650 kg/m3, and the initial stress of the inclined cables was also considered.

The figure below (Figure 1) presents the computational model diagram of the bridge, and Table 1 provides the main vibration frequencies and modal characteristics of the bridge. Figures 2 and 3 show the mode shapes of some significant frequencies.

Table 1. Structural Dynamic Characteristics

Mode Order	Frequency (Hz)	Mode Characteristics
1	0.15659	Main bridge main beam vertical deflection
2	0.28334	Main beam first-order symmetric lateral bending
3	0.4178	Main beam first-order symmetric vertical bending
4	0.48181	Main beam second-order anti-symmetric lateral bending + tower lateral deflection
5	0.50167	Main beam second-order anti-symmetric lateral bending + tower lateral deflection
6	0.70632	Main beam second-order anti-symmetric lateral bending + edge span first-order lateral bending
7	0.7068	Main beam second-order anti-symmetric vertical bending
8	0.82069	11# symmetric outward bending
9	0.82484	10# symmetric inward bending
10	0.84268	Main beam second-order anti-symmetric lateral bending + tower transverse bridge bending
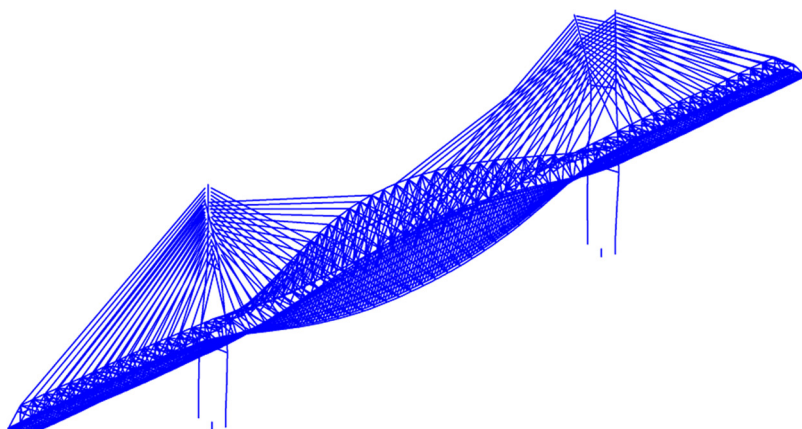
Fig. 1. Structural Finite Element Computational Model

Fig. 2. First symmetric lateral bending
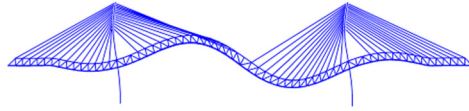
Fig. 3. First anti-symmetric vertical bending + vertical deflection.

3   Aerodynamic Force Parameters

The aerodynamic parameters used in this bridge, such as the three-force coefficients and aerodynamic derivatives, are based on the values obtained from wind tunnel tests conducted earlier. The three-force coefficients for the as-built condition of the bridge are listed in Table 2.

In the calculation of aerodynamic admittance, the structural damping ratio for the steel truss cable-stayed bridge is assumed to be 0.005. Three types of aerodynamic admittance functions are used:

The first type does not consider the effect of the aerodynamic admittance function, which means the aerodynamic admittance function is set to 1.

The second type adopts the Sears aerodynamic admittance function for lift and moment:

$$|\chi(k)|^2 = \frac{1}{1+\pi k}, \qquad k = \frac{\omega B}{U} \tag{1}$$

The third type utilizes the aerodynamic admittance functions derived from the study of the Balinhe River Extra Large Bridge:

Lift admittance function:

$$|\chi_L(k)|^2 = \frac{1.331}{1+1.737k^{0.616}} \tag{2}$$

Drag admittance function:

$$|\chi_D(k)|^2 = \frac{1.286}{1+2.99k^{0.574}} \tag{3}$$

Moment admittance function:

$$|\chi_M(k)|^2 = \frac{0.394}{1+0.003k^{3.413}} \tag{4}$$

Here, k represents the reduced frequency, B denotes the bridge width, and U represents the mean wind speed.

A comparison of various aerodynamic admittance functions is shown in Figure 4.

Table 2. Three-Force Coefficients and Slopes for Various Attack Angles in the Body Axis System

| Attack Angle (degrees)	C_D	C_L	C_M	C_D'	C_L'	C_M'
-5	0.79666	-0.38116	-0.05322	-0.35667	0.465815	-0.00201
-4	0.78329	-0.37294	-0.05382	-0.41138	0.463523	-0.05529
-3	0.7823	-0.36498	-0.05515	-0.2289	0.84941	-0.0762
-2	0.7753	-0.34329	-0.05648	-0.01518	1.890761	-0.10227
-1	0.78177	-0.29898	-0.05872	0.200822	3.135512	-0.06331
0	0.78231	-0.23384	-0.05869	0.480425	5.415597	0.11717
1	0.79854	-0.10994	-0.05463	0.902409	6.840257	0.378152
2	0.81381	0.00493	-0.04549	0.474409	5.921232	0.965147
3	0.8151	0.09675	-0.02094	0.115451	7.149081	1.122138
4	0.81784	0.25448	-0.00632	0.560066	9.517115	1.003536
5	0.83465	0.42896	0.01409	0.13264	8.532774	1.207509
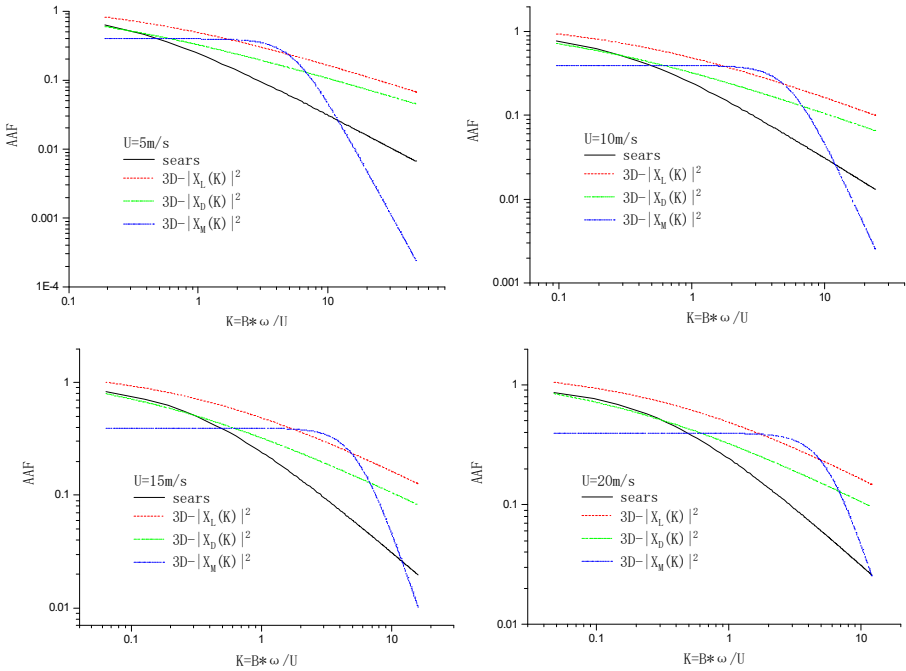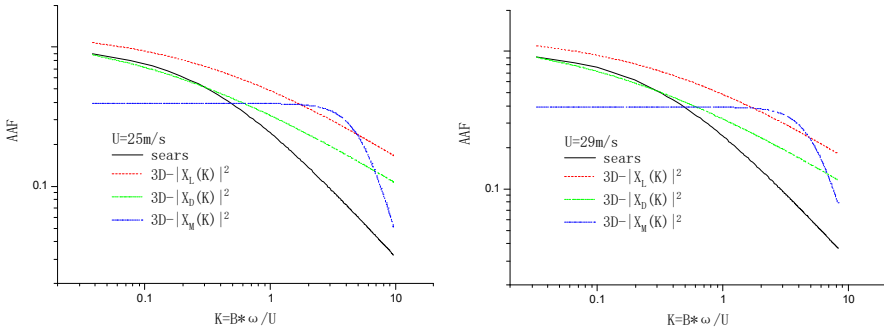
Fig. 4. Comparison of Different Aerodynamic Admittance Functions

4   Simulation of Random Wind Field

The simulation of the random wind field at the height of the main beam of the Hanjiatuo Yangtze River Bridge was conducted using the harmonic synthesis method. The wind field was simulated using the equivalent wind spectrum method. The simulation parameters are provided in Table 3, and the simulation results can be seen in Figure 5 and Figure 6.

Table 3. - Parameters for Simulating Turbulent Wind Speed

Bridge Span	864m	Cutoff Frequency	4π
Height of Main Beam from Ground	69m	Fraction of Frequencies	2048
Surface Roughness	0.22m	Sampling Time Interval	0.04s
Average Wind Speed at the Main Beam	29.0	Number of Simulated Samples	8192
Number of Simulation Points	65	Horizontal Wind Spectrum	Simiu spectrum
Spacing between Simulation Points	13.5m	Vertical Wind Spectrum	Lumly-Panofsky spectrum

Due to the lack of observed data on strong wind fluctuation time history at the bridge site, the wind spectrum and coherence function at the bridge site are expressed using commonly used forms from international sources. The lateral and longitudinal wind speed spectra adopt the Simiu spectrum, which varies with height, while the vertical wind speed spectrum adopts the Lumley-Panofsky spectrum.

Simiu Spectrum for Lateral and Longitudinal Wind Speeds

$$\frac{nS_u(f)}{u_*^2} = \frac{200f}{(1+50f)^{5/3}}, \quad \frac{nS_v(f)}{u_*^2} = \frac{15f}{(1+9.5f)^{5/3}} \tag{5}$$
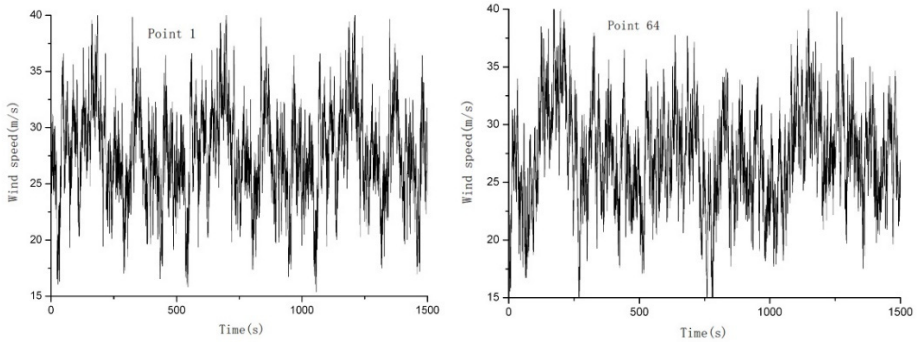
Lumley-Panofsky Spectrum for Vertical Wind Speed

$$\frac{nS_w(f)}{u_*^2} = \frac{3.36f}{(1+10f)^{5/3}}$$

(6)
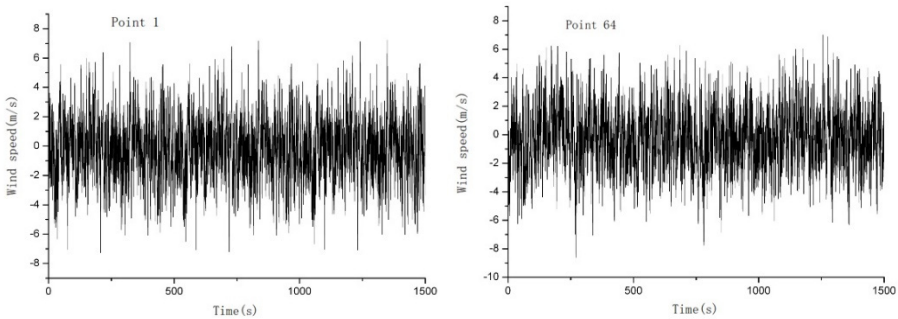
Where: f - Monin-Obukhov coordinate, n - frequency, u* - friction velocity.

The coherence function is expressed in the Davenport form:

$$Coh_{jm}(\omega) = \exp\left(-\lambda\frac{\omega r_{jm}}{2\pi U_Z}\right)$$

(7)

Where: λ - dimensionless attenuation factor, conservatively taken as 7; U_Z - mean wind speed at height Z; r_{jm} - distance between points j and m.

Fig. 5. Partial Time History of Horizontal Wind Speed at Simulation Points 1 and 64

Fig. 6. Partial Time History of Vertical Wind Speed at Simulation Points 1 and 64

5   Comparison of Frequency Domain and Time Domain[10-11]

Analysis for Flutter Frequency domain flutter analysis typically considers atmospheric turbulence as a stationary random process. Based on the wind speed spectrum and

considering the transfer function of the bridge structure, statistical quantities of flutter response are obtained. Frequency domain flutter analysis is simple and practical, but it is only applicable within the linear elastic range and does not provide the time history of structural response. Time domain flutter analysis, on the other hand, obtains time-domain wind loads based on simulated wind velocity fields, performs numerical integration of the structural dynamic equilibrium equation, and then calculates the structural response at each time step. Time domain flutter analysis is a simulation analysis that conveniently considers various influencing factors but requires a larger computational workload for numerical integration. With the improvement of computer performance, time domain analysis methods have been widely applied.

To examine the feasibility and reliability of time domain analysis methods for bridge flutter analysis and to validate the flutter analysis function of the bridge research analysis software RBAS, a comparison was made between time domain flutter response analysis and frequency domain flutter response analysis for the Hanjiatuo Yangtze River Bridge on the Yuli Line.

To compare with the frequency domain flutter analysis, the time domain flutter analysis only considered the fluctuating wind velocity field along the main beam. The Newmark-β method was used for integration calculations in the time domain flutter response analysis, with a time interval of 0.04 seconds and a total of 8192 steps. Figure 7 shows the vertical flutter displacement responses at different locations along the main beam under the design wind speed. For the frequency domain analysis, the first 40 mode shapes were considered. The structural vibration mode, flutter response root mean square (RMS), and flutter response power spectral density function were compared.

Taking the vertical vibration of the main beam as an example, the vibration mode of the structure was compared. Figure 8 shows the vibration status of the entire main beam at different time steps under a wind speed of 29 m/s. From Figure 8, it can be observed that the vibration of the entire main beam is approximately in a symmetrical form, which is consistent with the fact that the vertical vibration mode of the bridge is in a symmetrical form (Table 1). This also indicates that the primary flutter response of the bridge is dominated by the fundamental mode.
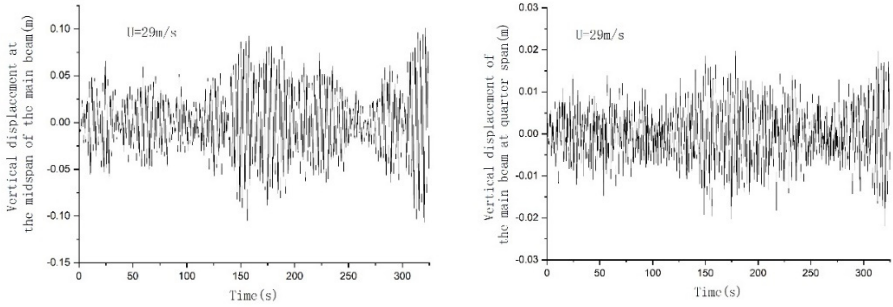
The variation of flutter displacement RMS at the midspan obtained from frequency domain and time domain analyses with wind speed is shown in Figure 9. It can be observed from Figure 9 that the time domain flutter response analysis results are slightly larger than the frequency domain results. Time domain analysis typically exhibits some level of discretization, and in this study, a relatively long calculation time was used (time interval of 0.04 seconds, with a total of 8192 steps).

The power spectral density functions of flutter displacement at the midspan obtained from frequency domain and time domain analyses are shown in Figure 10 (taking the left span as an example). It can be observed that the power spectral density functions obtained from the two methods (particularly the peaks corresponding to the natural frequencies) are reasonably consistent in both the vertical and horizontal directions, with slight differences in the high-frequency range.

The comparison of flutter analysis results between time domain and frequency domain from the aspects of structural vibration mode, flutter response RMS, and flutter response power spectral density functions indicates the following: (1) The time domain

flutter analysis method developed in this study is feasible. (2) Flutter displacement response of the bridge is typically dominated by the fundamental mode. (3) Time domain flutter analysis results exhibit some level of discretization and are slightly larger than the frequency domain analysis results. (4) Time domain flutter response analysis can reflect the contribution of higher mode shapes to the structural response.

Fig. 7. Time History of Vertical Flutter Displacement of the Main Beam
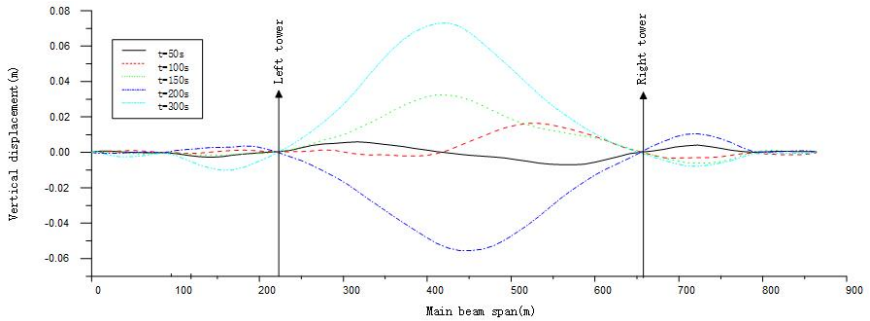
Fig. 8. Vertical Flutter Displacement of the Main Beam at Different Time Steps
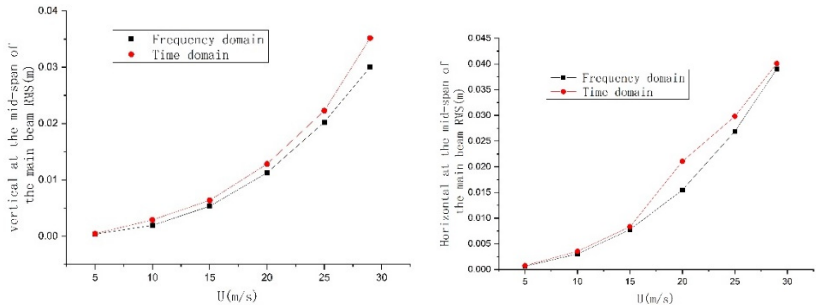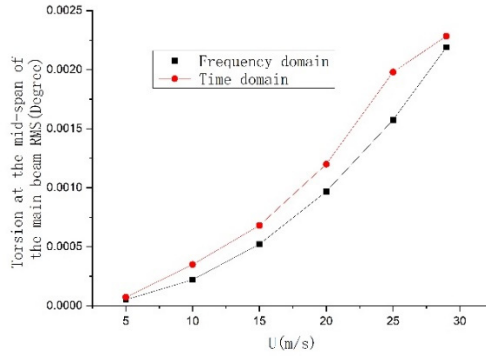
Fig. 9. Variation of RMS Value of Flutter Displacement at Midspan with Wind Speed
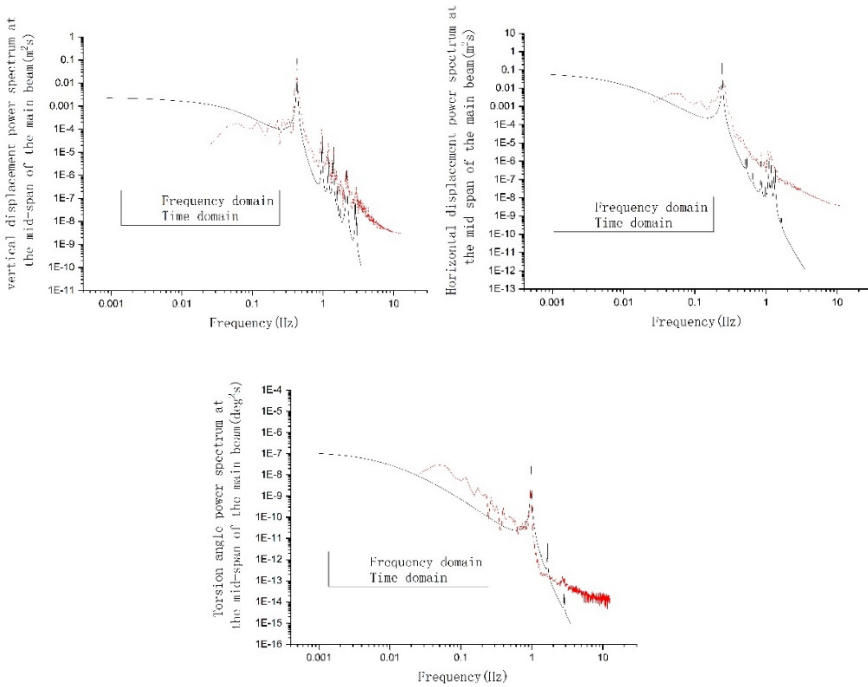
Fig. 10. Flutter Displacement Response Spectrum at Midspan

6   Conclusion

Through the time domain and frequency domain analysis of flutter using different aer-odynamic admittance functions for large-span railway cable-stayed bridges, the

influence of aerodynamic admittance on the flutter of bluff body bridges was systematically analyzed, leading to the following conclusions:

(1) The influence of aerodynamic admittance on flutter is significant. It can reduce the amplitude of flutter, suppress flutter occurrence, attenuate vibration propagation, and improve the stability of the bridge.

(2) The variation trends of aerodynamic admittance with reduced frequency are generally consistent at different wind speeds.

(3) For steel girder structures, the Sears function is less applicable, and the calculated results tend to be unsafe.

(4) Aerodynamic admittance has a significant impact on flutter response. The flutter displacement response considering the aerodynamic admittance function is noticeably smaller than the results without considering it. Therefore, the influence of aerodynamic admittance should be considered in the calculation and analysis.

Acknowledgment

7   References

1. Chen Z. Q. (2005) Bridge wind engineering. People's Transportation Publishing House, Beijing. pp.1 - 133.
2. Wang L.M., Shu H.M., Huang X. G. (2015) FEM Analysis of Pipeline Subject to Transverse Landslide Based on the Strain Criterion. Journal of Jiamusi University, 33:532-534
3. Zheng Y.F., Zhao Q., Bao W. (2018) Wind resistance performance of long-span continuous rigid-frame bridge in cantilever construction stage. Journal of Jilin University (Engineering and Technology Edition), 48: 466-472
4. Guo S.L., Zhong T.Y., Yan Z.G. (2021) Calculation of method of buffeting response for stay cables of long-span cable-stayed bridge. Journal of Jilin University (Engineering and Technology Edition), 51: 1756-1762.
5. Liao H.L., Li M.S., Ma C.M. (2020) State-of-the-art review of bridge wind engineering in 2019. Journal of Civil and Environmental Engineering, 42: 56-66.
6. Shen Z.F., Li J.W., Wang F. (2020) Buffeting response characteristics of the double main girder section suspension bridge with variable slot width ratios. Journal of Vibration Engineering, 33: 824 -833.
7. Tao T.Y., Wang H. (2019) Time-Domain simulation And analysis of nonstationary buffeting responses of girder section model of a long -Span bridge. Journal of Vibration Engineering, 32: 830 -836.

8. Sankaran R, Jancauskas E.D. (1992) Direct measurement of the aerodynamic admittance of two-dimensional rectangular cylinders in smooth and turbulent flows. Journal of Wind Engineering and Industrial Aerodynamics,1:41-44.
9. Larose G.L., Mann J. (1998) Gust loading on streamlined bridge decks. Journal of Fluid and Structure, 12:511-536
10. Ma C. M. (2007) Study on three-dimensional pneumatic admittance of streamlined box bridges. Southwest Jiaotong University, Chengdu. pp: 30-60
11. Xiang H.F. (2005) Modern Theory and Practice on Bridge Wind Resistance. China Communications Press, Beijing. pp:1-104